

A DIRECT ENERGY CONVERTOR FOR
UW TANDEM MIRROR REACTOR*

PFC/JA 80-33

*Work supported by DOE Cont.#DE-AC02-80ER-52057

A DIRECT ENERGY CONVERTOR FOR UW TANDEM MIRROR REACTOR

By T. F. Yang

Plasma Fusion Center

Massachusetts Institute of Technology

and

Walter Maurev

Fusion Research Program

Department of Nuclear Engineering

The University of Wisconsin

1. Introduction

In a Tandem mirror reactor, the end loss ions can be preferentially leaked out one end and hot electron out the other. A single stage regular Plasma Direct Converter (PDC) at the ion end to recover the ion power, and a simple thermal dump at the electron end, were considered by the reactor design team at LLL.⁽¹⁾ Such a converter has the net efficiency of 64% and would be as high as 77% if the 3.5 MeV α -particles can be recovered, which is the largest single loss. Another large loss is due to energy spread. A very important question, the neutron steaming out the ends, was not addressed in that design. In this study, an attempt was made to find solutions to these problems.

In Section 2, we discuss the method of designing the magnetic structures such that adequate space can be provided to shield the neutrons. The magnetic fluxes can be divided into small bundles so that the entrance grids and repeller grids could be eliminated.

The single stage direct converter will be considered as base case and discussed in Section 3. The advantages of two-stage converter is also discussed. Sections 3 and 4 discuss the vacuum requirement and efficiency.

2. Magnetic Systems

The magnetic flux lines out the ends of the TMR beyond the circularizing coils with regular single stage direct energy converter, is shown by Figure 1.⁽¹⁾ The neutrons and 3.5 MeV alphas streaming out the ends will impinge on the center section of the converter. This will increase the thermal load on the converter, cause damage, and reduce the efficiency. To shield neutrons and to prevent the alphas from reaching the collector, a solenoidal coil is added on the axis to divert the flux lines as shown by Figures 2 and 3. The shielding material can be placed in the private flux area inside the separatrix. The current carried by the solenoid is only 0.5 MA-T. Figure 4 shows the flux configuration when another solenoidal coil with current of same magnitude but of opposite direction is added. Figure 5 shows the flux for three solenoidal coils with alternate current directions. These figures demonstrated that the fluxes can be divided into many narrow annals of flux tubes or bundles, as are illustrated by the end views in Figure 6. By properly biasing the structure of the conducting rings, the entrance grids and the repeller grids can be removed.

The use of such a method for TMR, without circularizing coil, has also been investigated. The cross-section of the flux for such a TMR is elliptical. In principal, one can use picket fence arrangement instead of solenoids as shown by Figure 7. The structure for such a system may be simpler. However, it is difficult to find a reasonable flux configuration. Figure 8 shows the flux pattern with a single race track coil. The private flux lines

spiral inward, which can not yet be explained. This could be a numerical problem, inadequacy of the race track coil or non-uniform distribution of the magnetic flux of the original elliptic cross-section. More study has to be carried out to understand this method. For the present, we choose to use solenoidal coils with recircularized flux tube.

The results given in Figures 2-5 are the first successful calculation. Obviously, they can be optimized in many ways, such as moving the solenoids further out into the weaker field region to reduce the current requirement and varying the relative positions to obtain optimum configurations. However, the concept to divide and divert the flux for shielding the neutron, and for the electron stripping, has been demonstrated. In all these figures, the flux distribution, at a distance of about 10 meters away, is not changed by the solenoids; therefore, a spherical dish antenna type collector can still be used.

The cross-sectional areas of the coil shown in the figures are all $40 \text{ cm} \times 50 \text{ cm}$. Since the current in each coil is only 0.5 MA-T , a considerably smaller conductor can be used. If we choose a current density of 2 k amp/cm^2 , then the conductor size is only $16 \text{ cm} \times 16 \text{ cm}$. The shielding thickness is about 80 cm , which is quite adequate. This shield can be used as thermal dump for the 3.5 MeV alphas. The high energy alphas have a gyroradius of 10 times larger than 350 keV ions and more magnetically rigid. Therefore, the diversion of flux has small effect on these alphas so that they will dump their energy to the shield. The estimated surface area of the dump is about 7 cm^2 . The alpha power is 36 MW , which gives a heat load of 0.5 kw/cm^2 .

3. Single Stage Collector

The single stage convertor is illustrated by Figure 9. The convertor consists of ion collectors at high positive voltage (320 keV), the electron repeller grids at -35 keV , and entrance grid at -1 keV . The repeller grids prevent electrons from reaching ion collector. The cold electrons are reflected and collected on the entrance grids, which have to handle the heat generated by the electrons and the small fraction of ions impinging on the grids. The heat load on the entrance grid is greatly reduced due to the preferentially leaking of electrons through the other end.

Because of the circularizing coil, the flux tube has a circular cross-section, and the field lines radiate outward to form an expanding cone. The grids and collector of the PDC should be formed into the surface of spherical dish in order to intercept the ion at nearly normal incidence. Such a dish antenna type of structure is shown by Figure 10. The ion loss current for UWISTMR is $7.739 \times 10^{21} \text{ (D+T)/sec}$ and alphas is $0.43 \times 10^{21} \text{ /sec}$. The minimum energy is 325 keV and average ion energy is 350 keV . The ion and alpha power are 443 MW and 71 MW respectively. To handle 443 MW of ion power, the surface area of the dish collector

would be 14 m^2 to reduce the average power density to 300 W/cm^2 . The span of the dish is very large and the largest tube could be as long as 10 m if the seven section hexagon structure is used. Therefore, an octagon structure as is illustrated by Figure 11 is chosen. This will not only reduce the tube length, but also reduce the stored energy in each section, and give better approximation to a spherical dish. The current density on the collector is $j \simeq 8.6 \text{ amp/m}^2$. The spacings d_{max} can be determined by solving the child's law⁽¹⁾

$$d_{\text{max}}^2 = \frac{4\epsilon_0}{9} \sqrt{\frac{2q}{M}} \frac{v^{3/2}}{j_i},$$

where $\epsilon_0 = 8.85 \times 10^{-12} \text{ f/m}$, q is the charge and M is the mass of the ions and v is the voltage difference across the space d_{max} . One obtains $d_{\text{max}} \simeq 1.3 \text{ m}$, thus $d = 1.0 \text{ m}$ can be chosen. The stored energy for this system becomes

$$E_{st} = \frac{1}{2} \left(\frac{\epsilon_0 A}{d} \right) V^2 = 95 \text{ J}$$

The stored energy per section is less than 10 J , which can be released in a spark. According to Barr,⁽¹⁾ the grid voltage can be determined from Spangenberg's graph for a Triode to be -35 keV .

If we approximate the outer circumference of the octagon by πL , then the relation between L and ℓ for a given A is

$$\left(\frac{\pi}{4} / \cos \theta \right) L^2 = A - \frac{\pi}{4} \left(1 - \frac{1}{\cos \theta} \right) \ell^2$$

choosing $\ell = 2 \text{ m}$ and $\theta = 45^\circ$ and for $A = 144 \text{ m}^2$, one obtains $L = 10 \text{ m}$. Thus,

$$d_o = 4.7 \text{ m}$$

and

$$d_{in} = 0.83 \text{ m}$$

The longest tube length is only 5 m , which is much easier to handle. In principal, one can further divide each section into smaller modules. However, it is very difficult to subdivide the repeller grid and entrance grids because they have to be supported by cantilever through the collector. The support has to be well insulated. The cantilever will also be used as walter manifold. Further division will reduce the grid transparency and thus reduce the efficiency.

It is most desirable to eliminate these two structures. The method to accomplish this is to use the flux bundling method as illustrated by Figure 11. There are two flux annals. The total area of these two annals is 3 m^2 . The width of the annals is about 25 cm . The ion current density going through these annals is 413 amp/m^2 or 41.3 mA/cm^2 , which is comparable to the ion current density in a typical neutral beam designed for TFTR by ORNL and LBL.⁽²⁾ They are 61 mA/cm^2 and 90 mA/cm^2 respectively. The corresponding beam sizes are 2.5 cm in diameter and $10\text{ cm} \times 40\text{ cm}$. Therefore, the in beam direct energy conversion methods developed for the beam line can be applied to the TMR. Assuming infinite plasma in the circumferential direction of the flux annal and in the direction of the flux, the voltage required for stripping the electron can be estimated from⁽²⁾

$$V^- > (ja^2/8\epsilon_0v) \cdot (2b/a - 1)$$

$$> 35\text{keV}$$

assuming the electrode distance b , equals the plasma sheath thickness a . Here, v , is the ion velocity for 350 keV . This value is very reasonable. A secondary electron suppressor grid may still be needed and should be investigated. However, the suppressor grid was not used in the neutral beam. The -35 keV bias at the solenoidal coils may be sufficient. The self-field due to the ion space charge will spread out the ions further apart, which will further reduce the heat load on the collector or the collector can be more compact.

The minimum energy of the ions is 325 keV , the collector voltage is set at 320 keV to prevent the reflection of some ions. The high energy ions will impinge the collector with excess energy of 35 keV , thus increasing the heat load and reducing the efficiency. Two stage collector should be considered. The advantages of such a system are twofold. Besides increasing the efficiency and reducing the load, it will help the pumping requirement. This is illustrated by the two stage collector in Figure 13.

The ions with energy greater than 320 keV and less than 320 keV , will be reflected and collected at the 323 keV electrode. The high energy ions will be collected by the 355 keV electrode. The neutrals will be scattered by the first electrode and trapped behind the collector which can be pumped away. There is no danger of charge exchange and recombination problems on the backside so that it can be operated at high pressure. This enables the use of mechanical pumps to remove the neutrals.

Since the particles impinge on the grid at very high energy, the sputtering yield is very low (less than one tenth of a percent), Molybdeum coated copper tubing with 2 mm thick wall can be used for both grid and

collector for better heat transfer. Because of low heat load and with the use of copper tube, one may be able to recover a reasonable fraction of the thermal energy.

4. Vacuum Considerations

The pumping requirement for a single stage collector is briefly discussed in the following. To prevent the recombination and charge exchange of ions Barr⁽¹⁾ also estimated that the allowed pressure should be less than 3×10^{-5} Torr. The gas throughput is about 50 Torr-litres/sec, then the required pumping speed is

$$S = \frac{Q}{P} = 1.6 \times 10^6 \text{ litres/sec.}$$

Therefore, 36 m^2 of cryopanel is needed for a pumping speed of $4.4 \text{ litres/cm}^2\text{-sec}$ for a mixture of D_2 and T_2 gas at 300 k. The He throughput is $Q_{\text{He}} \approx 1.7 \text{ Torr-litres/sec}$. The pumping speed required for helium removal is

$$S = \frac{Q_{\text{He}}}{P} = 5.6 \times 10^4 \text{ litres/sec.}$$

Then He can be removed by a turbo-molecular pump. To maximize the conductance, the pump can be installed right next to the chamber.

5. Estimate of Efficiency

The efficiency of the PDC can be estimated by considering the losses. They are discussed in two categories. The negligible losses which are:

- (1) The loss due to cold electron is insignificant because the hot electrons are lost out the other end.
- (2) The residue field at the collector is only 0.05 T. This residue field does not limit the parallel energy at the collector, thus causes no loss of recovered power.
- (3) The pressure in the collector chamber is below 3×10^{-5} Torr, the loss of fast ions due to charge exchange is negligible. The power consumption on the repeller grid is negligible for the base design. For the advanced design, there is no repeller grid; therefore, no loss.
- (4) Because of large size and short length of the tube for repeller grid and collector, the coolant pumping loss power is negligible.

The accountable losses are:

(1) There is about 10% of loss due to the interception by the grids for the base design, but no loss for the advanced design.

(2) For the base design, the repeller grid is maintained at $V_g = -35$ kV by a power supply that must supply 64 amp of ions ($\sim 5\%$) and 192 amp for three secondary electron per incident ions. This amounts to a power loss of 9 MW or 2% of the incident 443 MW ion power.

(3) The collector voltage is designed at 320 kV. The average ion has 357 keV of energy and impacts the collector with excess 37 keV, giving a loss of 9% in directly recovered power. Three percent of this power may be recovered through thermal cycle. This power loss may be reduced to 4% for two stage collector.

(4) The collector voltage is set at 320 keV to off-set 8° deflection, this gives a loss of 2% of recovered power.

Therefore, the overall efficiency for regular single stage collector is 77%. It may be as high as 87% for the advanced design. Some of the α power may be recoverable at dump which will improve the efficiency.

6. Conclusion

It is proven here that a neutron shielding and α particle dump can be designed for a single stage regular collector with the efficiency of 77%. This shielding and dump will greatly improve the life of the collector.

It is also demonstrated that the flux tube out of the end of TMR can be divided into concentric flux annals; thus, the cold electron can be stripped with nominal voltage on the diverting solenoidal coils. This enables the elimination of entrance and repeller grid and thus greatly simplifies the collector structure and improves the efficiency. Further optimization of this concept should be done.

7. Acknowledgement

This work is performed for the Fusion Program of the University of Wisconsin under contract number UAJ 08HM604-1. The discussion with G. A. Emmert is enlightening. The help of Jack Tracey on the collector design and the drafting of C. Milonas are acknowledged.

References

1. W. L. Barr, UCRL-52836
2. G. W. Hamilton, "A 120 keV Beam Direct Conversion System for TFTR Injectors." LLL report UCRL-52137 (1976)

Figure 1

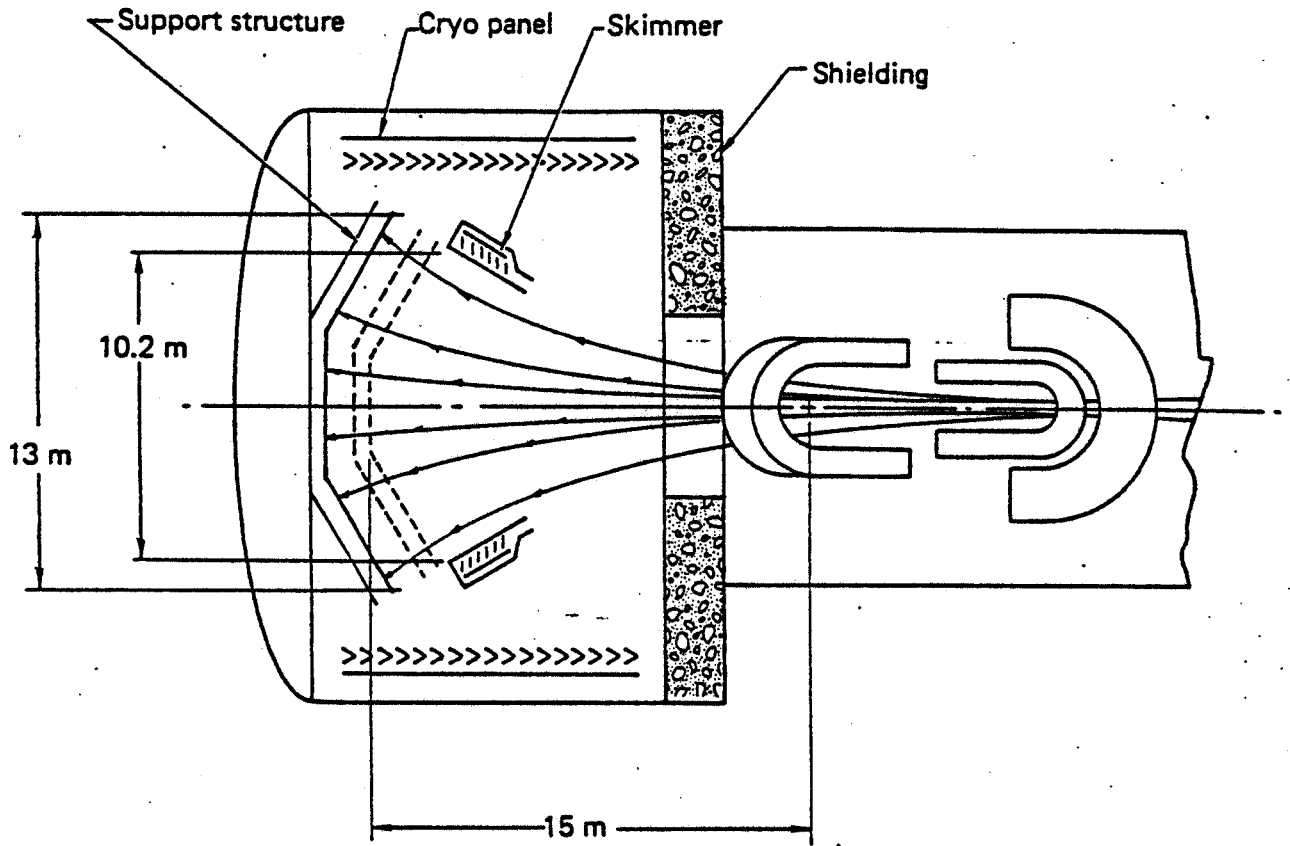
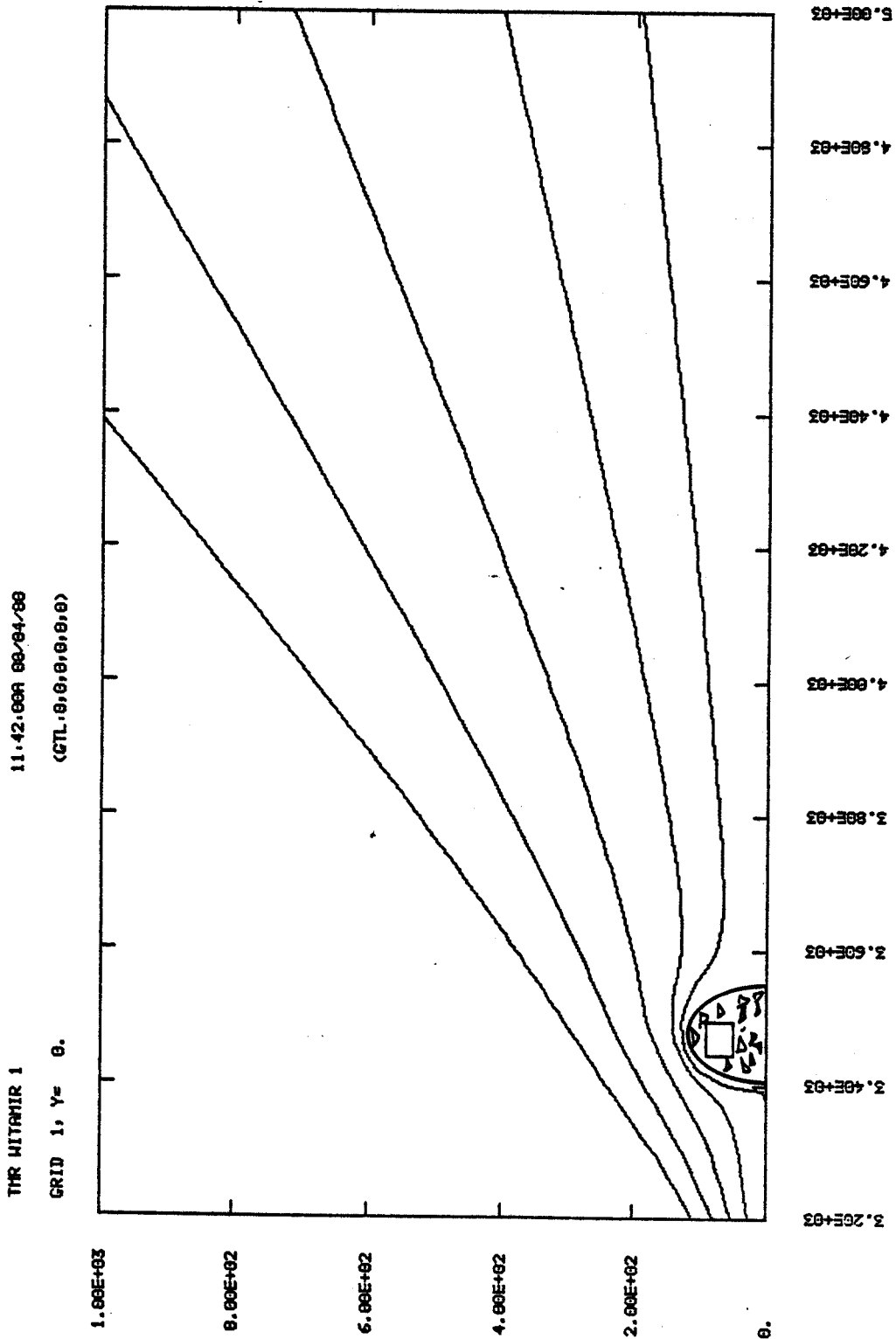


Fig.1. LLL-Single stage regular direct energy convertor

Figure 3



Z

Fig. 3. Diverted magnetic flux lines with one diverting coil out of the end of TMR

Figure 4

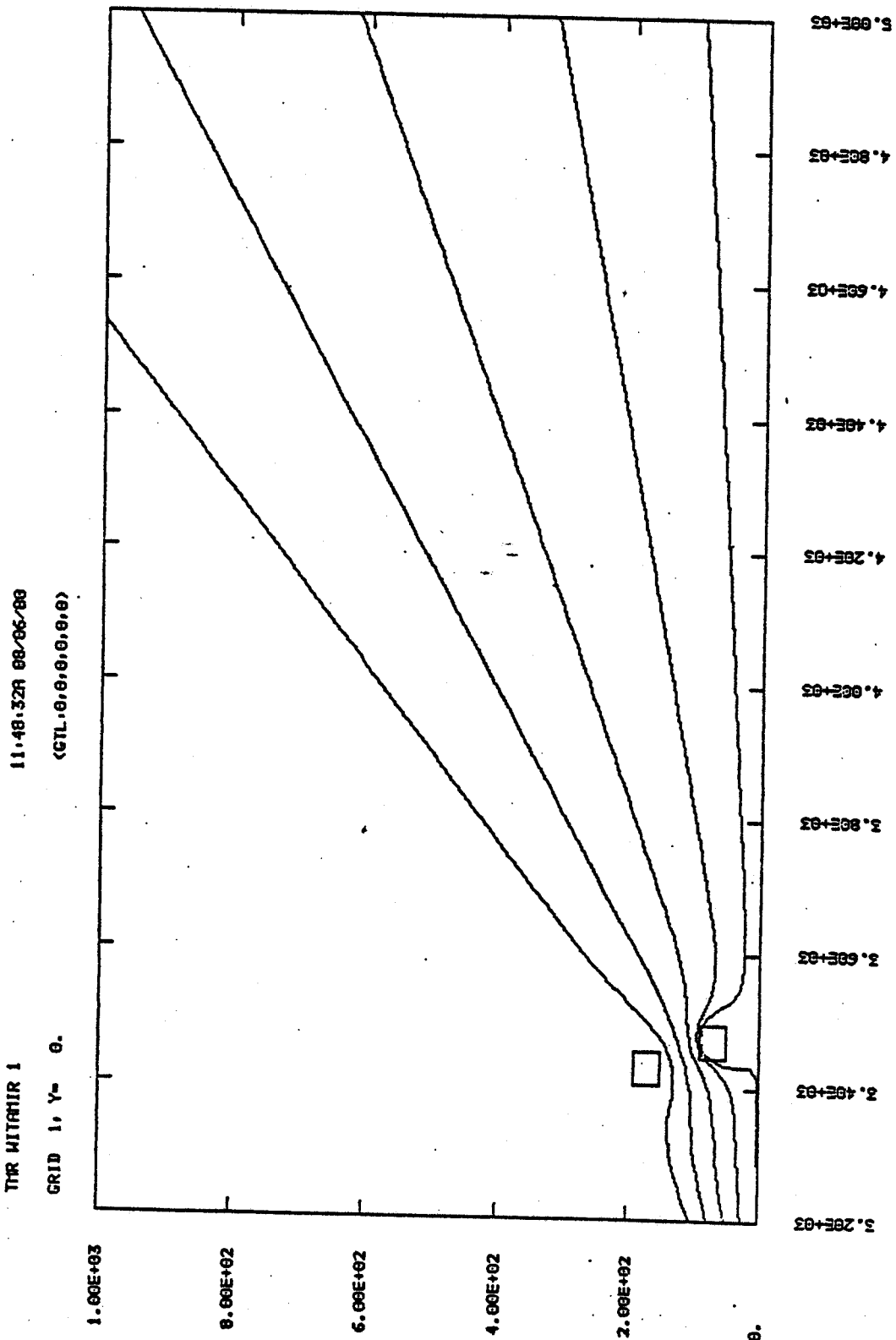


Fig.4. Flux lines for 2 diverting solenoidal coils

Figure 5

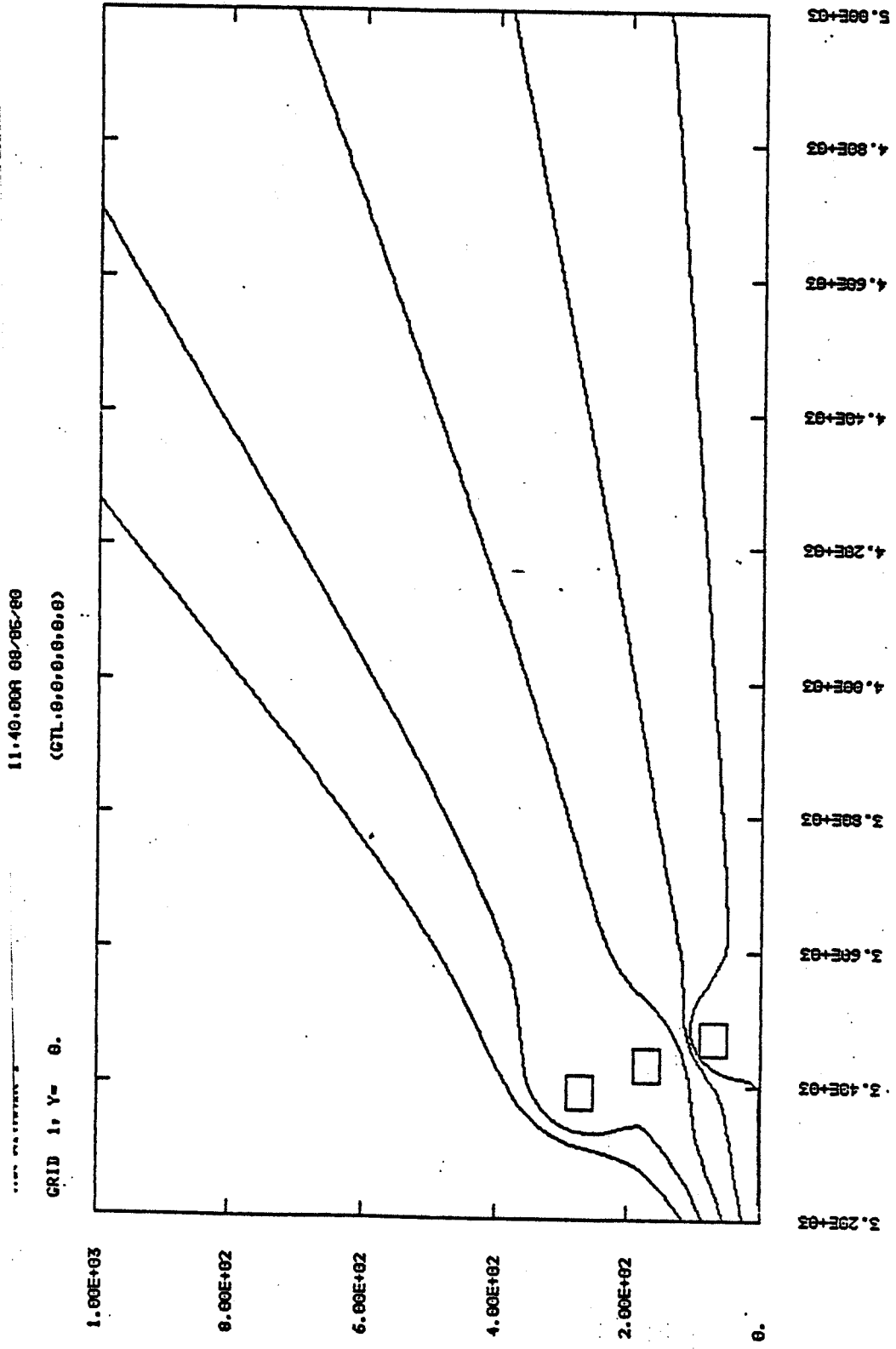


Fig.5. Flux lines for 3 diverting solenoidal coils

Figure 6.

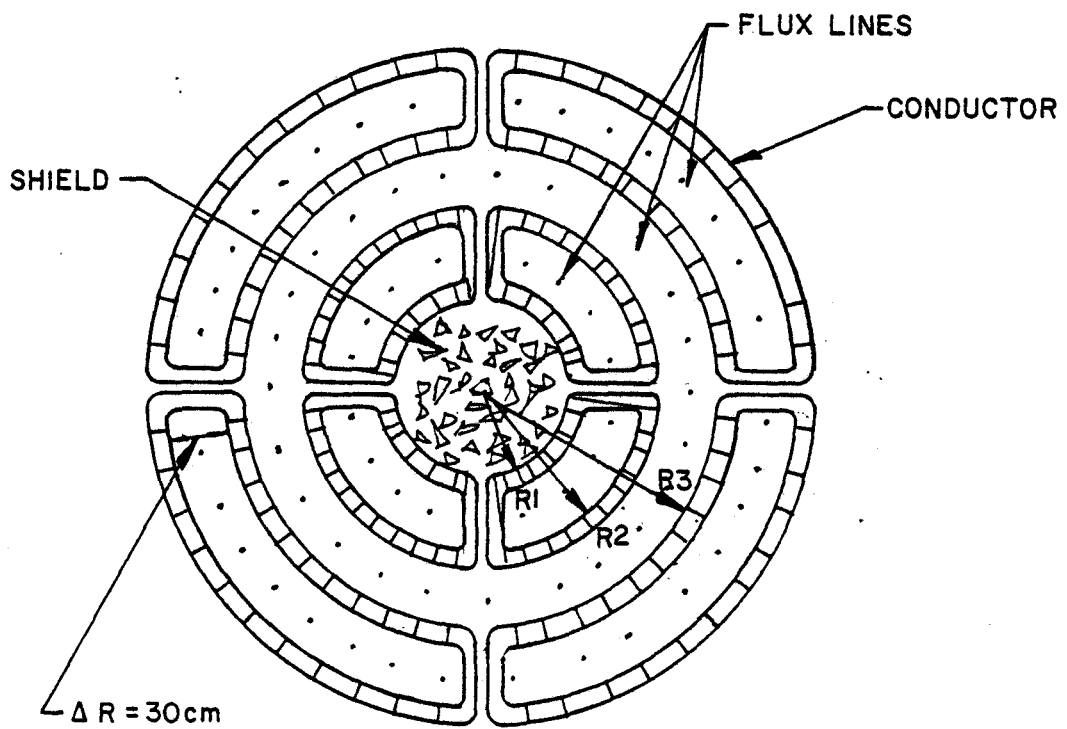
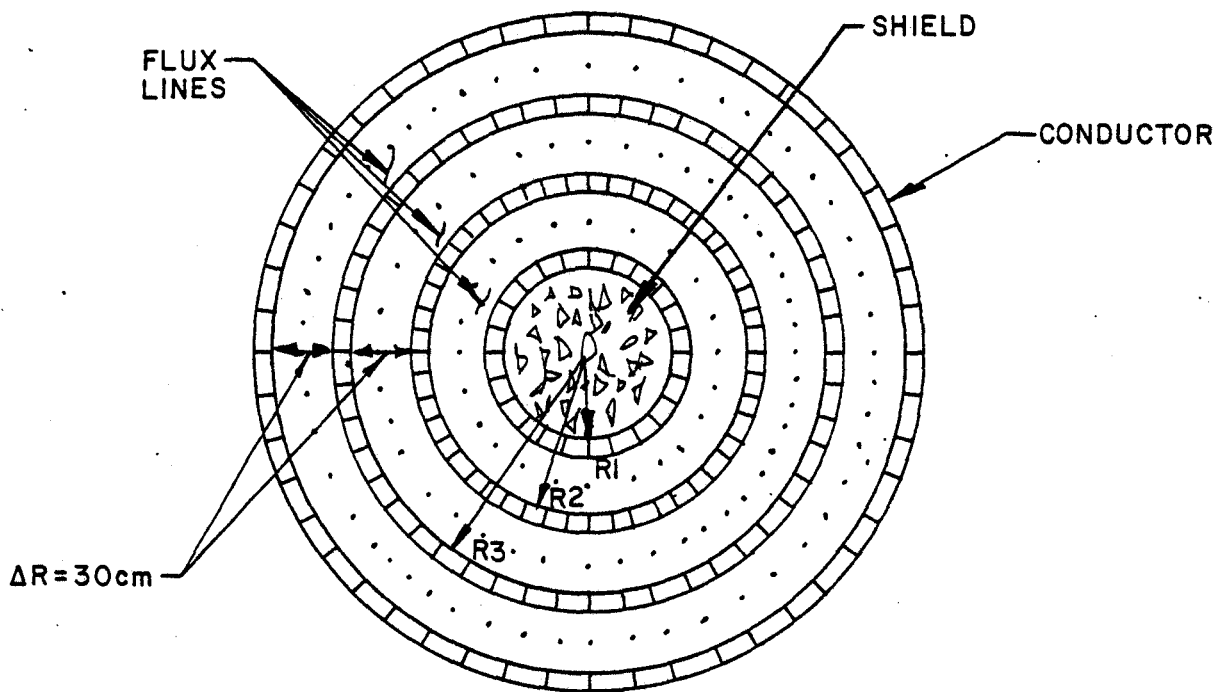


Fig.6. End views of flux bundling solenoidal coils. The bottom picture shows the segmentation of the coil pairs.

Figure 7

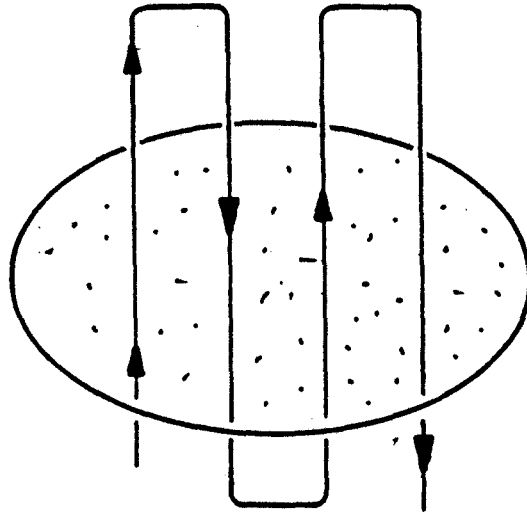


Fig.7. Picket fence diverting coils for elliptical cross-section flux tube out the end of TMR without recircularizing coils.

Figure 8

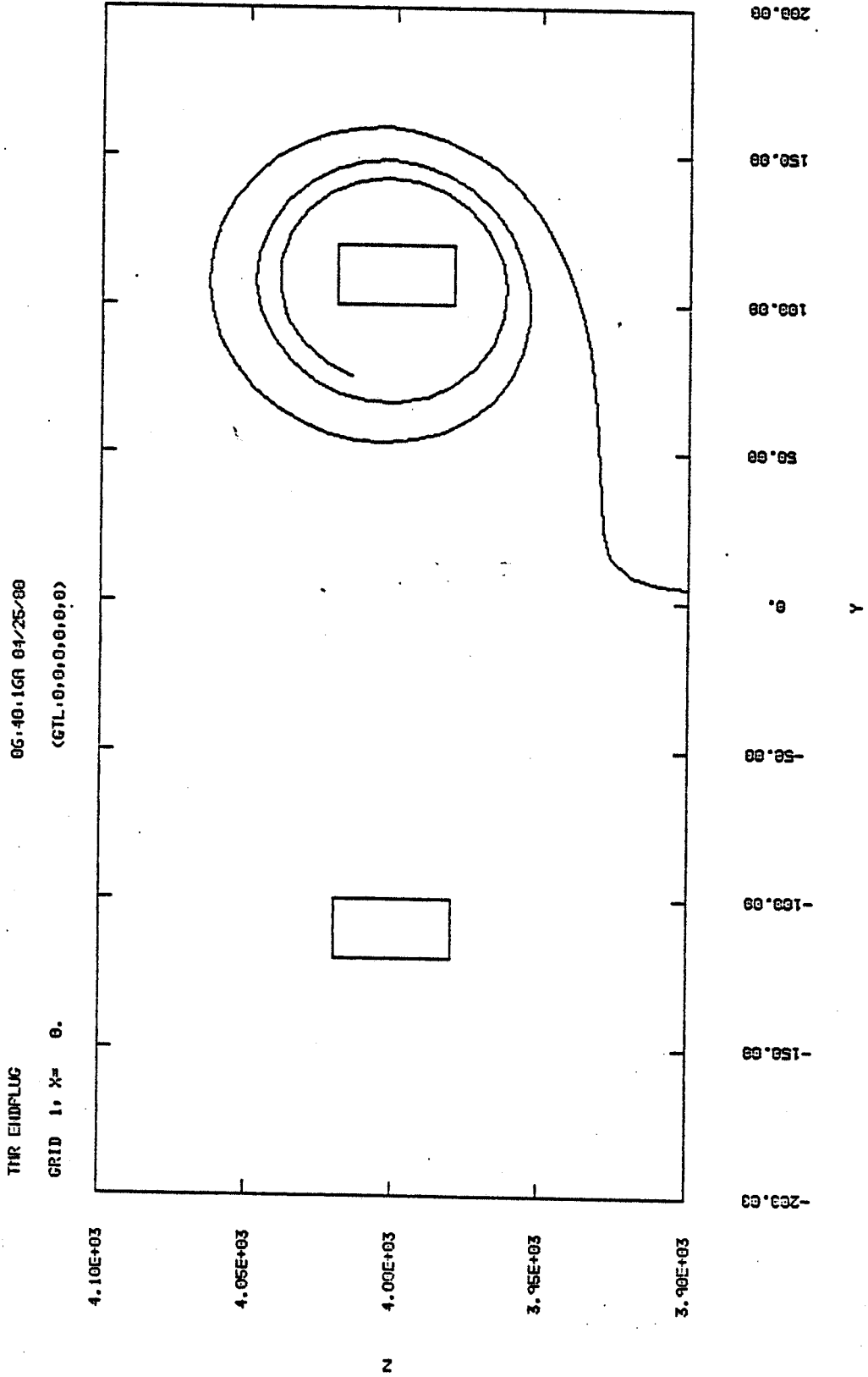


Fig.8. Flux lines for a single race track coil

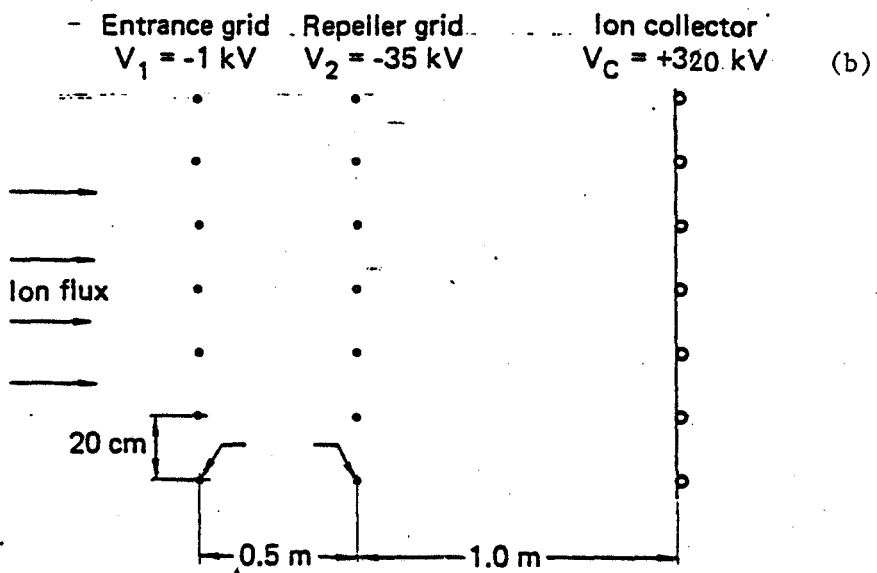
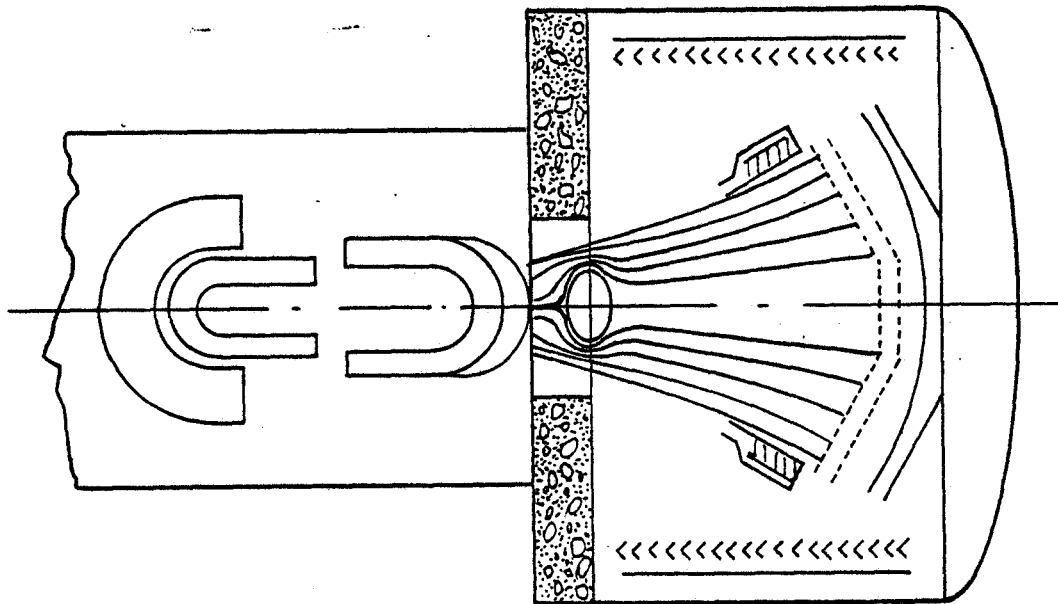


Fig.9. Single stage direct converter with one solenoidal diverting coil for TMR with recircularizing coils (a). and the grids and collector (b).

Figure 10

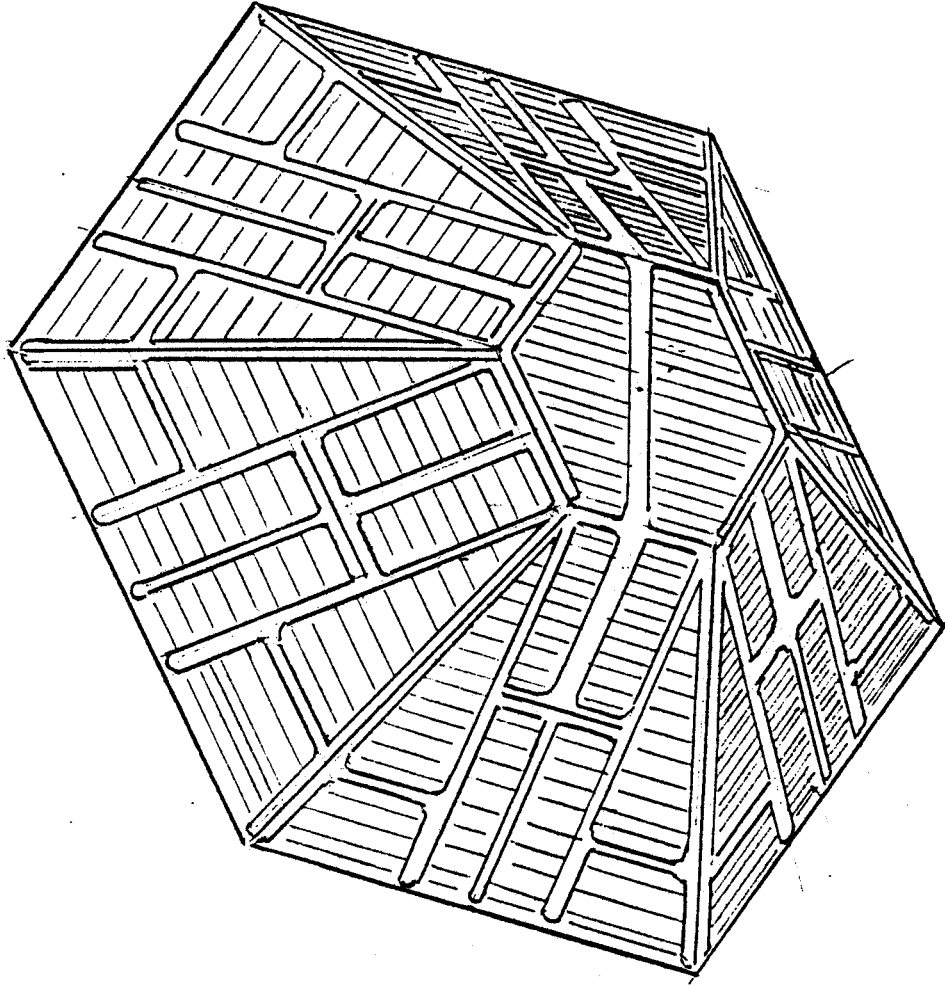


Fig.10. Dish antenna type of collector with hexagon shape

Figure 11

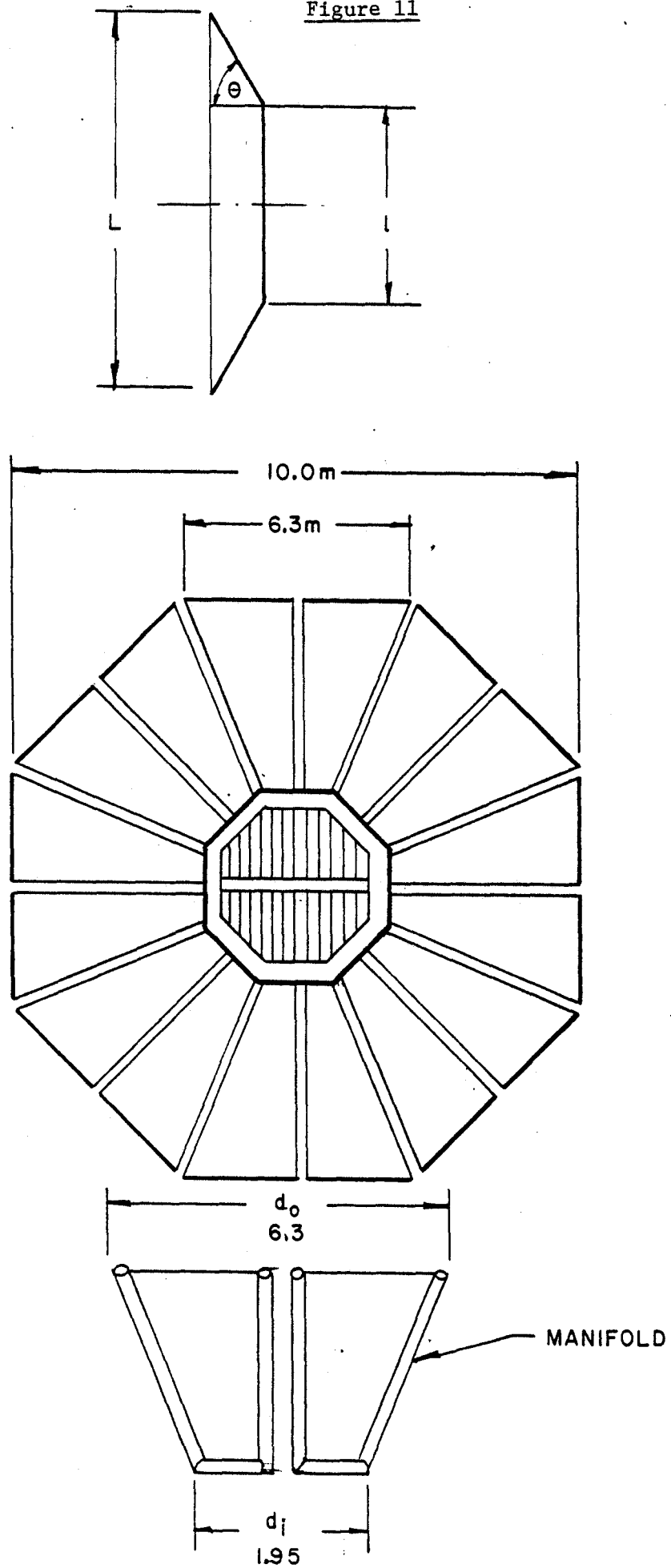


Fig.11. Octagon shaped collector. The collector is divided into 18 sections

11.40.00R 08/05/89

(CTL:0,0,0,0,0,0)

THR HITAIR 1

GRID 1, Y= 0.

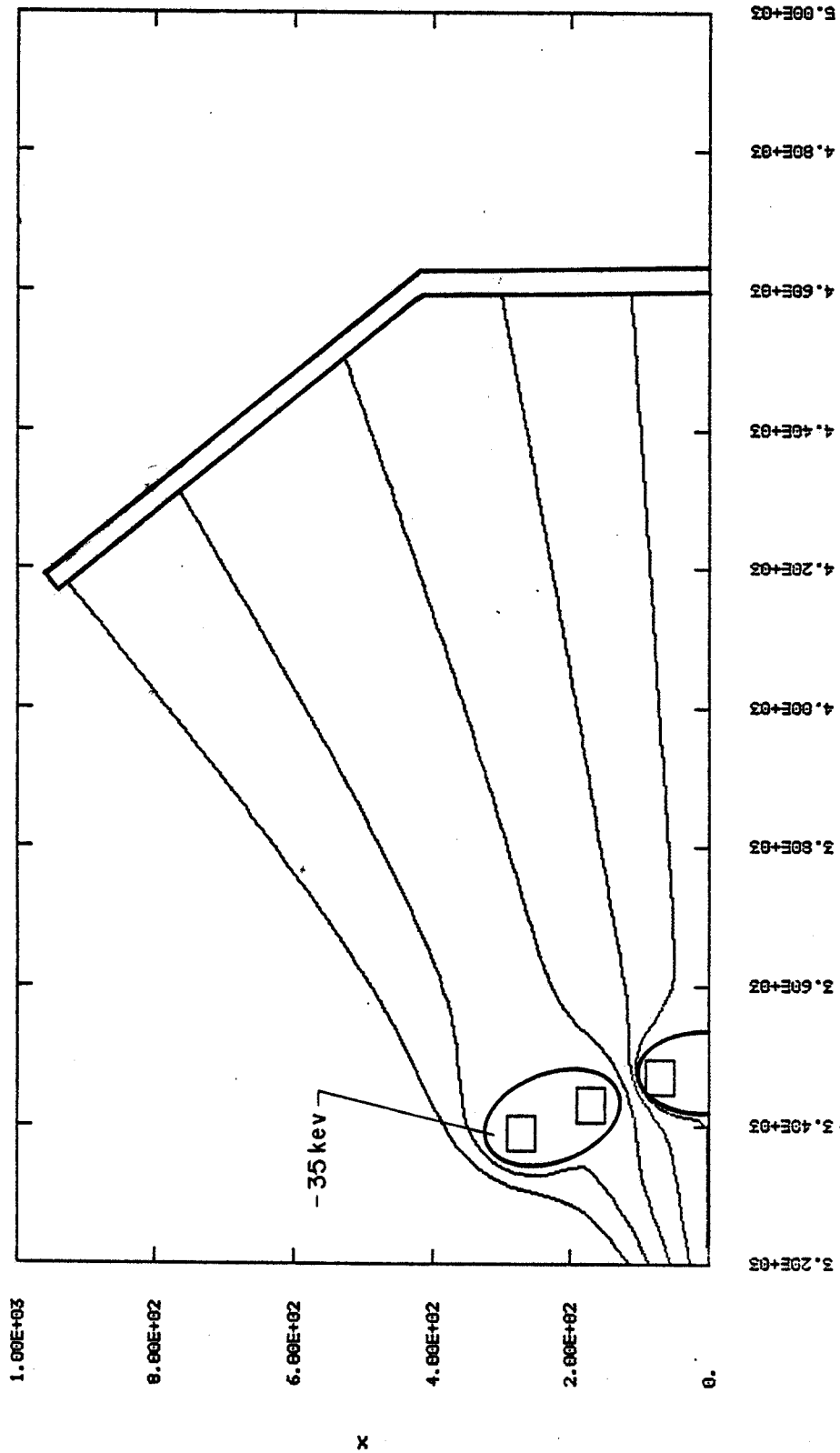


Fig. 12. Direct energy conversion system with three diverting coils. The coils are biased at 35 keV to strip cold electrons.

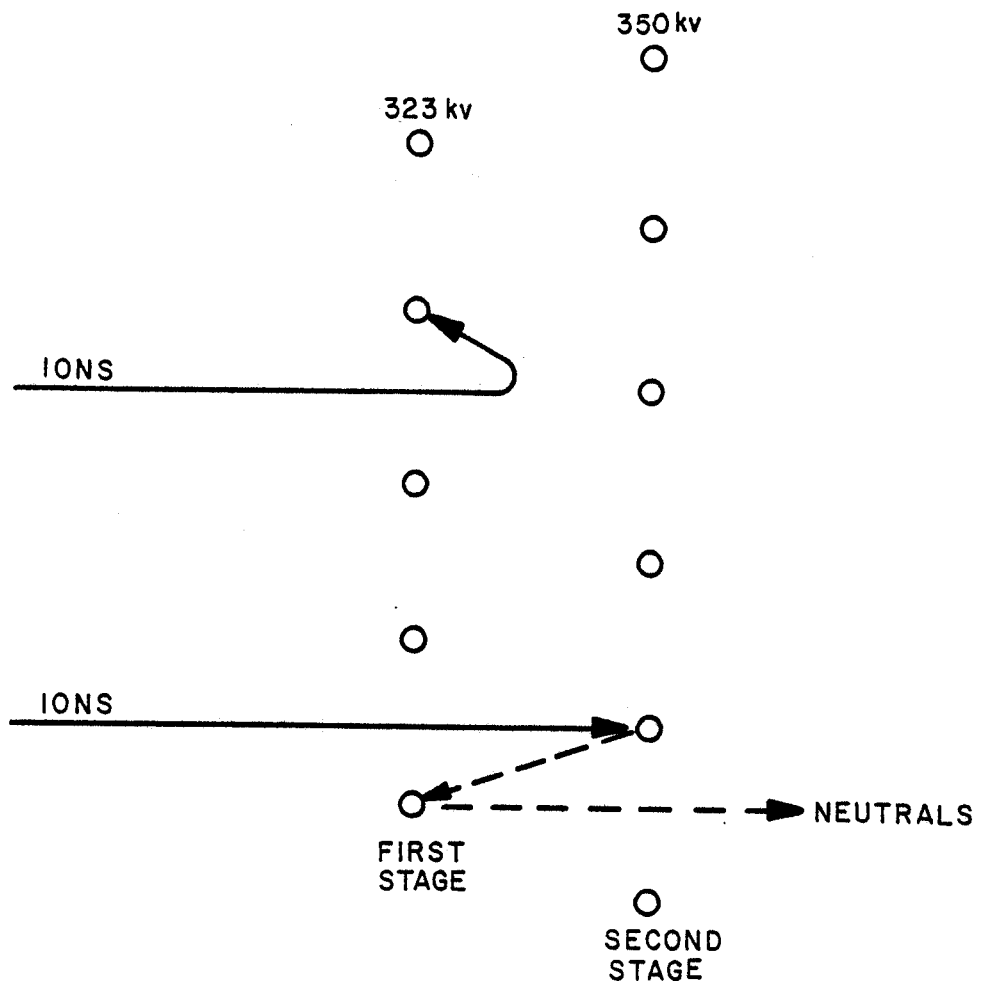


Fig. 13. A two stage collector concept.